Nigerian Research Journal of Engineering and Environmental Sciences 8(1) 2023 pp. 39-47
p ISSN: 2635-3342; e ISSN: 2635-3350

Nigerian Research Journal of Engineering and Environmental Sciences
Journal homepage: www.rjees.com

Original Research Article

Mechanical and Wear Performance Enhancement of a 3D-Printer Nozzle Fabricated from Millscale-Modified Copper-Zinc Alloy

***Sekunowo, O.I., Agboola, J.B. and Oserei, L.F.**

Department of Metallurgical & Materials Engineering, Faculty of Engineering, University of Lagos, Akoka, Nigeria.
*osekunowo@unilag.edu.ng

http://doi.org/10.5281/zenodo.8093857

ARTICLE INFORMATION

Article history:
Received 16 May 2023
Revised 14 Jun. 2023
Accepted 15 Jun. 2023
Available online 30 Jun. 2023

Keywords:
Additive manufacturing
3D-Printer nozzle
Wear
Mechanical properties
Iron-millscale
Copper-zinc alloy

ABSTRACT

The challenge of dysfunctional engineering components produced via additive manufacturing is a current global concern. This appears to stem from the relatively poor mechanical performances often exhibited by 3D-printers nozzles produced from brass. The current study investigated the feasibility of enhancing the wear and mechanical properties of 3D-printers nozzles using iron-millscale modified copper-zinc alloy as a viable alternative. The methodology entailed addition of varying weight percent of iron-millscale (IMS) into copper-zinc alloy aimed at significantly modifying its microstructure for desirable impact on the mechanical properties. The charges were melted in an induction furnace, cast in metal moulds and characterised for wear and mechanical properties. Results show that the formulation containing 6 wt. % IMS addition exhibited superior mechanical characteristics in terms of hardness (201.4 VHN), wear rate (0.69 cm^2 x 10^{-6}), wear resistance (934.9 cm^{-2} x 10^3) and modest impact energy (30.3 J). These results compare well with desirable wear and mechanical properties of high quality 3D printer nozzles. Contributions to this level of performances may have emanated from the refined microstructure showing homogeneously dispersed fine $CuFe_3Zn_2$ crystals. It is concluded that the developed alloy is a viable candidate material for 3D printer nozzle production.

1. INTRODUCTION

Amongst other materials such as stainless steel and hardened steel, most three-dimension (3D) printer nozzles are made from brass owing to its great thermal conductive properties (Sukindar *et al*., 2017; Shakor *et al*., 2019; Carolo, 2020; Memar *et al*., 2023). However, due to the relatively low wear characteristics of brass, its usage

for producing 3D printer nozzle is limited to the printing of only relatively soft materials such as polylactide acid (PLA) and acrylonitrile butadiene styrene (ABS) (Melo *et al.*, 2022; Dizdar and Krishna, 2022). These materials are free from any hard additives such as glass, carbon fibres or metallic particles (Weng *et al.*, 2016; Zhang *et al.*, 2017). Discrimination against these materials is premised on the likelihood of forming grooves and ridges on the inner walls of the nozzle. It also predisposes the nozzle to clogging of its orifices rendering it unusable (Li *et al.*, 2017).

In spite of the utility value of copper-zinc alloy, there has not been any significant work done to modify its microstructure in a manner that enhances its wear characteristics and other desirable functional properties. It was reported that the mechanical properties of copper can be improved by alloying resulting in awesome thermal and wear characteristics (Chen *et al.*, 2021; Tezel and Kovan, 2022). However, the limitation imposed on the mechanical property enhancement of Cu-Zn by alloying necessitates additional alloy material which possesses the potential for property improvement that is devoid of debilitating structure compromise (Gibson *et al.*, 2021). As reported by Igelegbai *et al.,* (2017), the feasibility of the foregoing occurring depends on the addition of a material that has the propensity for structure modification in a manner that induces fine grain and coherent crystals within the copper matrix.

It has also been shown that the mechanical characteristics of 3D printers' nozzles impact significantly the quality of the printed products in terms of functionality and aesthetics. Excessive wear of the nozzle is often a precursor for irregular product dimensions and poor surface finish (Tezel and Kovan, 2022). Furthermore, inherent structure defects contribute majorly to deleterious mechanical properties of printed components hence, the need to ensure that 3D printer nozzles exhibit desirable level of hardness and wear resistance behaviours (Igelegbai *et al.*, 2017). In the recent technical review on zinc alloys microstructure and mechanical properties carried out by Pola *et al.*, (2020), it was projected that the use of zinc as alloy in brasses will continue to increase owing to its preferential applications in foundry technologies. Addition of zinc in copper is known to confer good mechanical property and better wear behaviour than conventional copper alloy (Igelegbai and Alo, 2015)). It was also reported that the mechanical properties of Cu-Zn alloy can be improved by adding small amounts of certain elements such as chromium, iron and nickel (Okayasu *et al.*, 2017).

Ironmillscale (IMS) is the flaky generic iron oxides (FeO, Fe_2O_3 and Fe_3O_4) resulting from oxidation of roll stocks during hot rolling of steel. The accumulation of IMS constitutes a huge waste to steel rolling mills with the attendant disposal challenges. Consequently, some innovative methods for a safe disposal of IMS are being developed. In addition, it has been established that IMS possesses a high propensity to nucleate ferritic structures in some non-ferrous alloys which enhances their mechanical properties (Bugdayci, *et al., 2018; Wang,* et al., 2021). Thus, the current study intends to employ iron-millscale to refine the parent copper-zinc alloy microstructure for enhanced mechanical properties in terms of wear, impact and hardness

2. MATERIALS AND METHODS

2.1. Materials

The materials used for this study are copper and zinc slabs sourced commercially at the metals section of Owode-Onirin market, Lagos while iron-millscale (IMS) was obtained from African Foundries Limited, Lagos, Nigeria (Figure 1a-c). The preparation of the materials involved oven drying of the IMS using an oven-dryer (model DHG-9030, Japan), ball millingwith the aid of a milling machine (model, JC-QM-2, China) and sieving to 150 µm while both slabs of copper and zinc were mechanically sliced into pieces to render them chargeable into the furnace before melting.

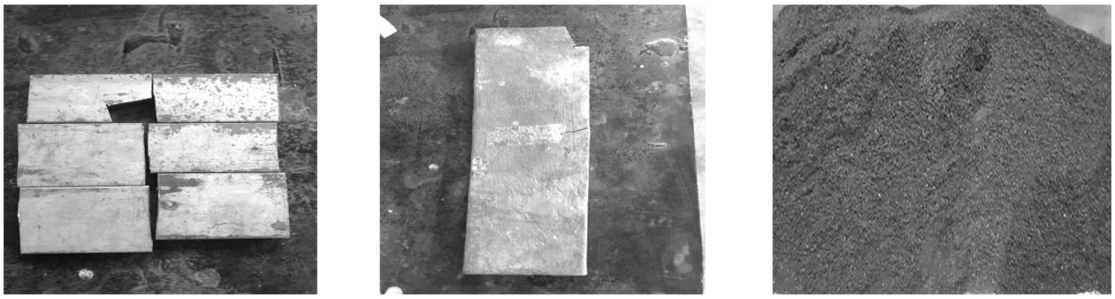

(a) (b) (c)

Figure 1: Research materials used (a) copper slabs (b) zinc slabs (c) pulverised and sieved IMS

2.2. Methods

2.2.1. Melting and casting

The materials were blended according to formulation shown in Table 1 while the IMS was added at varied amounts (6-12 wt. %) and stirred for 45 seconds on each addition. With reference to Ayeni (2018), after melting, the molten alloy was cast in metal moulds and kept for an hour at room temperature to age-harden artificially. Then, the cast samples were stripped from the moulds, fettled and trimmed.

Table 1: Material formulation

ID	Materials, wt. %		
	Cu	Zn	Millscale
Ac	70	30	0
B	70	18	12
C	70	20	10
D	70	22	8
E	70	24	6

2.3. Characterisation

2.3.1. Composition analysis

The materials used for the study were subjected to composition analysis using a metal analyser (Model, ARL 3460, Switzerland) while the IMS being compounds of oxides was analysed using X-ray fluorescence (XRF).

2.3.2. Microstructural analysis

All the test specimens were prepared according to relevant ASTM E407 standards (2016). One sample from each composition was subjected to both optical and scanning electron microscopy. Optical microscopy (OM) test specimens were prepared by grinding using emery papers of 1000 µm grade and polished using polishing powders to obtain mirror-like surfaces. Ferric chloride ($FeCl_3$) solution mixed in 200ml and 50 ml distilled water was applied as etchant. The specimens' microstructural features were viewed under OM at 400 magnifications (x400). Scanning electron microscope (SEM) model, EVO LS10 manufactured by Carl Zeiss, Germany was also employed to reveal detailed features of the specimens.

2.3.3. Mechanical characterisation

The samples impact energy behaviour was evaluated using Charpy V-notched specimens prepared according to ASTM E23 standard (ASTM 2023). An Avery Denison impact tester, (model 6705, UK) was employed to obtain the specimens impact energy values. Hardness evaluation was conducted on 10 x 10 mm specimens shown in Figure 2a while indentation of the specimen surfaces was done using a hardness machine (Model, Matsuzawa MMTX, Japan) (Figure 2b). The specimens polished surfaces were indented using a quadrangular diamond-shaped pyramid indenter under a load of 100 gf for 10 seconds dwell time. The Vickers indented area and hardness number were calculated using Equations 1 and 2.

$$A=\frac{d^2}{2\sin\left(\frac{136^0}{2}\right)} \quad (1)$$

d is the average length of the diagonal left by the indentation

$$\text{VHN} = \frac{F}{A}(kgf/mm^2) \quad (2)$$

Where F and A are the applied load over the indented area respectively

(a)

(b)

Figure 2: Pictures of (a) prepared hardness test specimens and (b) hardness tester

2.3.4. Wear characterisation

Wear test samples of 10 x 15 mm dimension were used to evaluate the wear characteristics of the developed alloy. The test was conducted on a pin-on-disc machine on which the sample was held stationary against a rotating wheel fixed with a 60-grit emery paper. The additional test parameters include a constant applied load of 11.38 N at 250 rpm rotating speed. The mass-loss in the test samples weight before and after applying the load at intervals of 30 s, 60 s and 90 s were obtained using a digital weigh scale and the data tabulated. Thereafter, the alloys' wear characteristics were computed using Equations 3 - 5.

$$\text{Wear volume} = mass\ loss / density \quad (3)$$

Where the alloy density was computed to be 8.2 gcm^{-3}

$$\text{Wear rate} = \frac{wear\ volume}{sliding\ distance,} \quad (4)$$

Where *sliding distance* $= \frac{2\pi RN}{60} \times time$ (s) and R (Radius of abrasive wheel = 7.25 cm and N (rpm) = 300)

$$\text{Resistance} = \frac{1}{wear\ rate} \quad (5)$$

3. RESULTS AND DISCUSSION

3.1. Chemical Composition

The results of the materials composition analysis are shown in Tables 2-3 respectively for copper (Cu), zinc (Zn) and IMS. Table 2a shows Cu as the main element with silicon (Si), iron (Fe) and Zn relatively substantial. Similarly, Zn concentration in Table 2b as aluminium (Al), Si, Fe and Cu presence are relatively significant. As shown in Table 3, the three generic iron oxides carry a large chunk of the IMS constituents. Generally, given the relative substantial presence of iron, silicon and tin in the research materials composition, the potential for structure modification resulting in mechanical property enhancement appears highly feasible (Huang and Hu, 2022).

Table 2a: Elemental composition of copper sample

Element	Cu	Si	Fe	P	S	Zn	Mo	Pb	Ti	Sn
Wt. %	71.89	2.95	0.46	0.06	0.05	0.56	0.01	0.03	0.43	23.56

Table 2b: Elemental composition of zinc sample

Element	Zn	Fe	Cu	Sn	Pb	Ni	Cr	Al	Mn	Si	P	S
Wt. %	79.42	0.63	2.87	0.02	0.51	0.03	0.02	6.56	0.09	9.72	0.06	0.07

Table 3: Chemical composition of iron-millscale by XRF

Compounds	Weight (%)
FeO	67.59
Fe_2O_3	24.16
Fe_3O_4	5.09
SiO_2	0.02
MgO	.0.05
CaO	0.18
MnO	0.03
Al_2O_3	0.01
*L.O.I	2.87

*L.O.I. = Loss on ignition

3.2. Microstructure

The optical micrographs of the developed alloys are presented in Figures 3(a-e). Starting with the monolithic copper micrograph (Figure 3a), the matrix is overwhelmingly filled with islands of dross-like zinc crystals in α-copper matrix. On addition of 12 wt. %IMS (Figure 3b), the $CuFe_3Zn_2$ crystals induced appears to be saturated with IMS. Coupled with the presence of 18 wt. %Zn, most of the crystals became coarse and dispersed in a segregated form. This feature is known to be a precursor to poor mechanical properties (Igelegbai *et al.*, 2017). Similarly, the addition of 10 wt. %IMS (Figure 3c) gave rise to the emergence of two phases with apparent thick grain boundaries which seem to partition the structure. This type of microstructural feature has been shown to induce weak inter-crystal cohesion giving rise to impaired mechanical properties (Igelegbai and Alo, 2015).

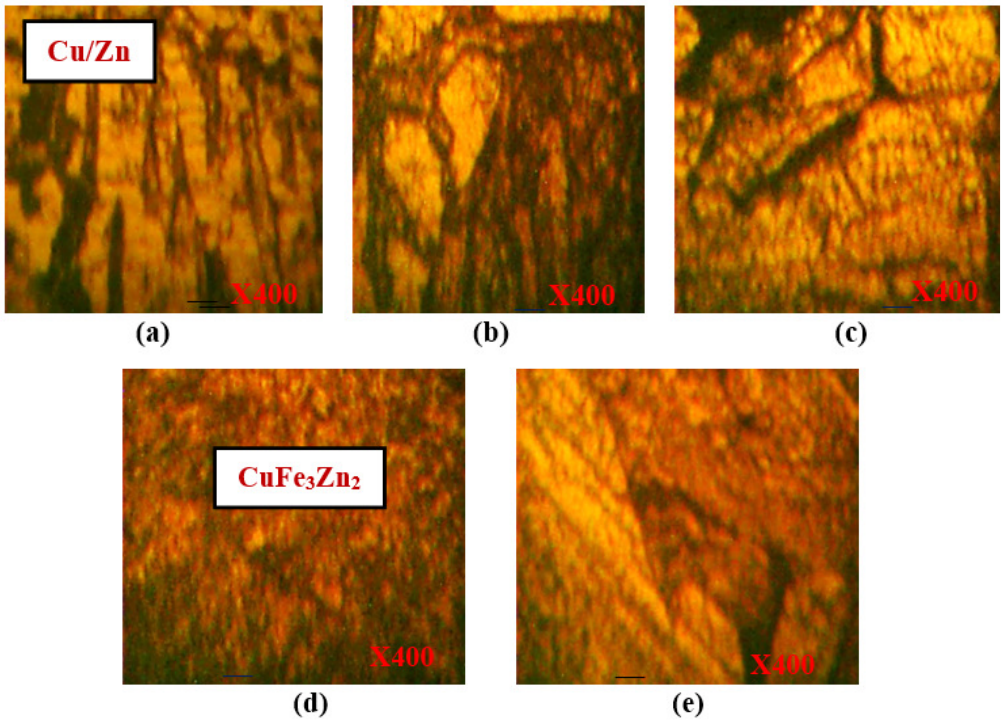

Figure 3a: Optical micrographs of the developed alloy at varied wt. %IMS addition (a) 0 (b) 12 (c) 10 (d) 8 and (e) 6

The optical micrograph shown in Figure 3d contains 8 wt. % IMS, which feature a rather subdued level of grain growth. Thus, the crystals appear relatively coarse but uniformly dispersed within the matrix. Figure 3e shows the micrograph developed on addition of 6 wt. %IMS. The crystals appear to be relatively fine and homogeneously dispersed in the matrix. It appears the IMS propensity to modify the Cu-Zn alloy microstructure

has been most effective at 6 wt. %IMS addition. This invariably may be taken as the optimum addition of IMS in the Cu-Zn binary alloy system. Thus, the property enhancement potential is expected to be optimum at this level. In order to further explore the alloy microstructural features, both the control sample (Figure 4a) and the 6 wt. %IMS (Figure 4b) were subjected to SEM analysis.

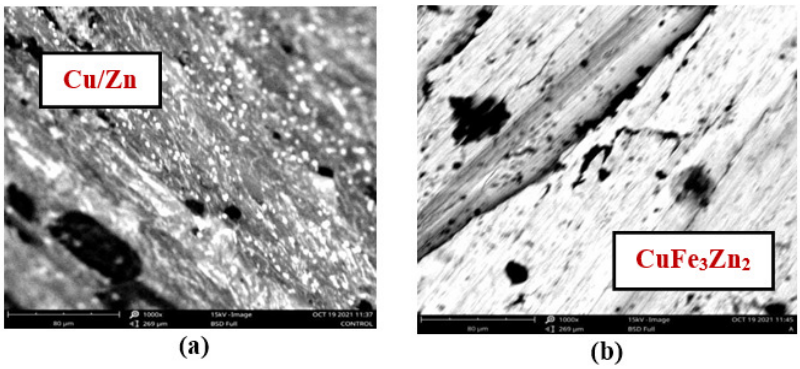

Figure 4: SEM micrographs of the developed alloy at varied wt. %IMS (a) 0 b) 6

3.3. Hardness

The hardness variation induced in the developed alloys is illustrated in Figure 5 demonstrating increase in hardness values in tandem with increasing IMS addition. The volume fractions of the fine $CuFe_3Zn_2$ crystals in the alloys microstructure may have been responsible for the observed trend. The highest hardness (201.7 VHN) occurred at 6 wt. %IMS addition occasioned by the plethora of grain boundaries induced in the alloy which may have enhanced its surface hardness. This level of hardness is adjudged to be sufficient in application such as 3D printer nozzle (Chen *et al*., 2021).

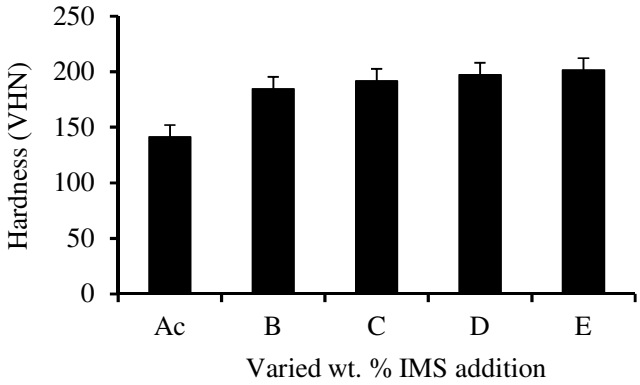

Figure 5: Hardness variation of IMS-modified Cu-Zn alloy

3.4. Impact Energy

Figure 6 depicts the impact energy variation of the IMS-modified Cu-Zn alloy. At lower IMS addition, impact energy first increased noticeably from 12.3 J to 22.5 J; after which, it tended to grow marginally as IMS addition increased. It is noteworthy that the microstructure of the alloy contains evenly distributed $CuFe_3Zn_2$ particles which enhanced proper matrix bonding giving rise to improved impact energy at low IMS addition. This corroborates the submission by (Pola *et al*., 2020). The modest rise in the impact energy values of the other compositions can be attributed to poor bonding caused by a seemingly excess IMS concentration.

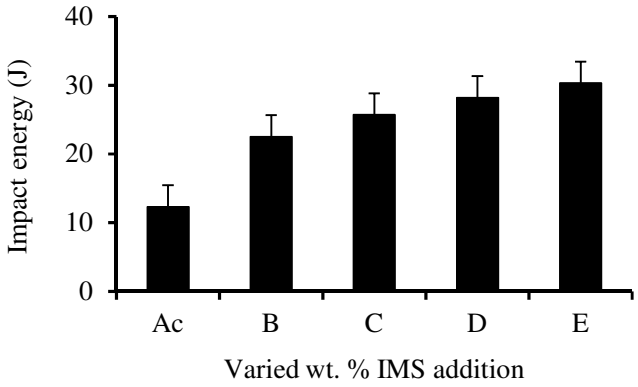

Figure 6: Impact energy variation of IMS-modified Cu-Zn alloy

3.5. Wear Characteristics

The wear characteristics of the developed alloy containing four different IMS addition is presented in Table 4 and illustrated in Figure 7. At shorter sliding time of 30 s, the rise in temperature between the sliding surfaces presumably may not be high enough to generate full oxide films, hence, the wear rate (1.05-1.88 cm^2 x 10^{-6}) at this stage is transient. As the sliding time is prolonged (60 s), the temperature between the sliding surfaces is sufficient to generate oxide films which tends to aid the recovery of the worn-out surface resulting in wear rate decline to 1.06-0.096 cm^2 x 10^{-6}.

Table 4: Wear characteristics data

SN	Sliding time (s)								
	30			60			90		
	V (cm^3. 10^{-2})	W_{Ra} (cm^2.10^{-6})	W_{Re} (cm^{-2}. 10^3)	V (cm^3.10^{-2})	W_{Ra} (cm^2.10^{-6})	W_{Re} (cm^{-2}. 10^3)	V (cm^3. 10^{-2})	W_{Ra} (cm^2.10^{-6})	W_{Re} (cm^{-2}. 10^3)
Ac	2.35	3.51	284.9	2.67	1.95	512.8	5.93	2.89	345.8
B	1.43	1.05	952.4	1.70	1.24	806.5	2.04	2.99	334.5
C	1.32	1.93	518.1	1.45	1.06	943.4	2.10	1.02	977.2
D	1.27	1.85	539..3	1.34	0.098	1016.1	2.78	1.36	736.4
E	1.28	1.88	532.7	1.31	0.096	1044..3	1.67	0.081	1227.6

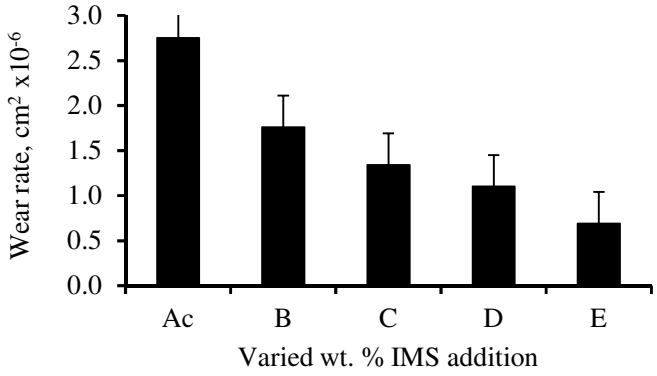

Figure 7: Wear rate of IMS-modified Cu-Zn alloy

However, at the long run (90 s sliding time), the oxide layer formed tends to reach a critical thickness, which becomes too weak to withstand the applied load resulting in a rather precarious high wear rate of 1.36-2.99 cm^2 $x10^{-6}$. These results indicate that sliding time, surface finish, applied load and microstructural integrity are critical factors that impact wear behaviour of engineering components (Memar *et al.*, 2023). According to Tezel and Kovan (2022), the microstructural integrity has overriding influence on wear behaviour.

4. CONCLUSION

Iron mill scale modified copper-zinc alloy was successfully produced. Generally, the addition of varied amount of IMS as structure modifier improved the mechanical properties and enhanced the wear characteristics. The formulation containing 6 wt. % IMS addition exhibited superior characteristics in terms of hardness (201.4 VHN), wear rate (0.69 cm^2 x 10^{-6}), wear resistance (934.9 cm^{-2} x 10^3) and modest impact energy (30.3 J). These results compare well with desirable wear and mechanical properties of high-quality 3D printer nozzles. Contributions to these levels of performances are attributed to the development of homogeneous and coherent fine $CuFe_3Zn_2$ crystals within the alloy matrix. It is concluded that the developed alloy is a viable candidate material for 3D printer nozzle production.

5. ACKNOWLEDGMENT

The authors wish to acknowledge the assistance and contributions of the laboratory staff of Department of Physics University of Lagos, Akoka, Lagos where the wear tests were carried out.

6. CONFLICT OF INTEREST

There is no conflict of interest associated with this work.

REFERENCES

ASTM E407 (2016). Standards Practice for Microetching of Metals and Alloys.

ASTM E23 (2023). Standard Text Methods for Notched Bar Impact of Metallic Materials.

Bugdayci, M., Alkan, M., Turan, A. and Yuceil, K. (2018). Production of Iron Based Alloys from Mill Scale through Metallothermic Reduction. *High Temperature Materials and Processes*, 37(9-10), pp. 88-98.

Ayeni, O. I. (2018). Sintering and Characterisation of 3D Printed Bronze Metal Filament. Master Thesis, Indianapolis, Indiana: *Advances* Purdue University, USA.

Carolo, F. (2020). Best 3D Printer Nozzle-Buyer's Guide. Available at https://all3dp.com.Accessed on March 30, 2023.

Chen, X., Bao R. Yi, J. Tao, J. and Li, F. (2021). Enhancing Mechanical Properties of Pure Copper-based Materials with Cr_xO_y Nanoparticles and CNT Hybrid Reinforcement. *Journal of Material Science,* 56, pp. 3062-3077.

Dizdar, S. and Krishna, A. V. (2022). Microstructural and Mechanical Properties of Polylactic Acid/Tin Bronze Tensile Strength Bars Additive Manufactured by Fused Deposition Modeling. *Advances in Multidisciplinary Engineering,* 21, pp. 566-579.

Gibson, I., Rosen, D and Stucker, B. (2021). Additive Manufacturing Technologies: Springer International Publishing; XXIII, 675.

Huang, S. and Hu, Q. (2022). Medium-Range Structure Motifs of Complex Iron Oxides. *Journal of Applied Physics,* 131(7), pp. 902-913.

Igelegbai, E. and Alo, O. (2015). Investigation of Mechanical Properties and Microstructure of Brass Alloys Obtained from Recycled Copper and Zinc Metals. *International Journal of Scientific and Engineering Research,* 6(9), pp. 799-813.

Igelegbai, E., Alo, O., Adeodu, A. and Daniyan, I. (2017). Evaluation of Mechanical and Microstructural Properties of α-Brass Alloy Produced from Scrap Copper and Zinc Metal through Sand Casting Process. *Journal of Minerals and Materials Characterization and Engineering,* 5, pp. 18-28.

Li, C; Cheng, W. and Hu, J. (2017). Nozzle Problem Analysis and Optimisation of 3D Printers. *Advances in Computer Science Research,* 75, pp. 270-273.

Melo, J; Santana, L; Idogava, H; Pais, A. and Alves, J. (2022). Effects of Nozzle Material and its Lifespan on the Quality of PLA Parts Manufactured by FFF 3D Printing. *Engineering Manufacturing Letters,* 11, pp. 20-27.

Memar, S; Azadi, M. and Abdoos, H. (2023). An Evaluation on Microstructure, Wear and Compression Behaviour of Al_2O_3 / Brass Matrix Nanocomposites Fabricated by Stir Casting Method. *Materials today Communications,* 34, pp. 105-123.

Okayasu, M; Muranaga, T. and Endo, A. (2017). Analysis of Microstructural Effects on Mechanical Properties of Copper Alloys.*Journal of Science: Advanced Materials and Devices,*2, pp.128-139.

Pola, A., Tocci, M. and Goodwin, F. (2020). Review of Microstructure and Properties of Zinc Alloys.*Metals,* 10(2), pp. 252-267.

Shakor, P; Nejadi, S. and Paul, G. (2019). A Study into the Effect of Different Nozzles Shapes and Fibre-Reinforcement in 3D Printed Mortar. *Materials,* 12 (10), pp. 1708-1730.

Sukindar, N; Ariffin, M; Baharudin, M; Jaafar, C. and Ismail, M. (2017). Analysis on the Impact of Process Parameters on Tensile-Strength using 3D Printer Repetier-Host Software.*Journal of Engineering and Applied Science,* 12 (10), pp. 416-427.

Tezel, T. and Kovan, V. (2022). Determination of Optimum Production Parameters for 3D Printers Based on Nozzle Diameter. *Rapid Prototyping Journal,* 28(1), pp. 184-194.

Wang, X; Jiang, J; Li, G; Shao, W. and Zhen, L. (2021). Particle-Stimulated Nucleation and Recrystallization Texture Initiated by Coarsened Al2CuLi Phase in Al-Cu-Li Alloy. *Journal of Materials Research and Technology*, 10, pp. 643-650.

Weng, Z; Wang, J; Senthil, T. and Wu, L. (2016). Mechanical and Thermal Properties of ABS/Montimorillonite Nano-Composite for Fused Deposition Modelling 3D Printing. *Materials Design,* 102, pp. 276-283.

Zhang, F., Ma, G. and Tan, T. (2017). The Nozzle Structure Design and Analysis for Continuous Carbon Fiber Composite 3D Printing. *Advances in Engineering Research,* 136, pp. 193-199.